LAWRENCE
LIVERMORE
NATIONAL
LABORATORY

LLNL-TR-414873

BIOCOMPATIBLE FLUORESCENT MICROSPHERES: SAFE PARTICLES FOR MATERIAL PENETRATION STUDIES

G. Farquar, R. Leif

July 17, 2009

Disclaimer

This work performed under the auspices of the U.S. Department of Energy by Lawrence Livermore National Laboratory under Contract DE-AC52-07NA27344.

BIOCOMPATIBLE FLUORESCENT MICROSPHERES: SAFE PARTICLES FOR MATERIAL PENETRATION STUDIES

DTRA Project BA06TAS416

Final Report

2009

George R. Farquar, and Roald Leif*

Lawrence Livermore National Laboratory, *Principal Investigator

Contents:

Abstract:

Biocompatible polymers with hydrolyzable chemical bonds have been used to produce safe, non-toxic fluorescent microspheres for material penetration studies. The selection of polymeric materials depends on both biocompatibility and processability, with tailored fluorescent properties depending on specific applications. Microspheres are composed of USFDA-approved biodegradable polymers and non-toxic fluorophores and are therefore suitable for tests where human exposure is possible. Micropheres were produced which contain unique fluorophores to enable discrimination from background aerosol particles. Characteristics that affect dispersion and adhesion can be modified depending on use. Several different microsphere preparation methods are possible, including the use of a vibrating orifice aerosol generator (VOAG), a Sono-Tek atomizer, an emulsion technique, and inkjet printhead. Applications for the fluorescent microspheres include challenges for biodefense system testing, calibrants for biofluorescence sensors, and particles for air dispersion model validation studies.

Introduction:

The use of biocompatible polymer microspheres has been proposed for use in drug delivery, dispersal model verification and as a surrogate for threat agents in instrument validation. The ability to have a polymer sphere with a broad range of property tuning will allow for safe low cost use for homeland security and defense applications. Three main challenges are present in the production of such spheres. The first challenge is the reproduction of the fluorescent and other chemical properties of interest. Secondly, the particles must have the size and charge attributes needed for the specific application and testing. Finally, in order to reproduce testing and evaluation criteria a rapid, reliable, scalable and low cost production method must be available

In order to simulate the fluorescent properties of threat agents several non-toxic biological chemicals are available that cover narrow emission ranges. Dipicolinic acid, tyrosine and tryptophan were evaluated for use to simulate a *B. anthracis* emission spectrum. Initial production of biosafe simulant microspheres at LLNL was done with an emulsion technique and a VOAG aerosol generator to combine the fluorophores tryptophan and poly-tryptophan.

The accurate and reproducible production of single size microspheres, or microspheres within a range of sizes, is important for reproducible studies and for rapid mass production since target bio-threats have specific size ranges determined by intrinsic properties and aerosolization and handling methods. If a sample particle has the correct chemical properties such as fluorescence but falls outside of the desired size range the particles may not be suitable as a simulant.

Aerosolization and the inherent chemical properties of particles will determine the ability to carry charge. If charge on a particle changes so do many critical properties. The settling time and filtration efficiencies of commercial air handling equipment can be effected by charge. At LLNL it has been determined that something as simple as a plastic air handling "jug" used in experiments can remove half of the charged particles. Unfortunately the charge on a plastic surface can vary with time and both positive and negative charged particles will be removed at different rates as the experiments progress. This is attributed to the particles being rapidly adsorbed by the charge on the plastic surface.

Finally, the stability of particles is critical for field studies. As particles age it is likely that the chemical nature and bio-simulant properties that are desired will change. If these changes are large the particle will no longer sever as an accurate bio-simulant.

The following sections are broken down under Measurements into experimental aspects or components of the overall study. Each area or section will focus on a set of measurements. The areas include experimental details and results with brief conclusions. This format is intended to allow for rapid identification and reference for an individual topic such as size determination or fluorescent properties.

Measurements:

Sphere Production:

In order to produce the base micro spheres three main methods were used. First, digital sonifier and sono-tech was used to produce polydispersed aerosol sizes. Secondly, a vibrating orifice aerosol generator (VOAG) was used to produce monodiperesed aerosols. Finally, inkjet print technology was used to produce aerosols with the possibility of large scale production and a narrow size distribution. An example of poly-dispersed spheres is shown in figure 1.

Pure polymer microspheres were synthesized using a Branson Digital Sonifier (Model 450. Three co-polymers, poly(DL-lactide-co-glycolide), avg. MW 5000-15000, DL-lactide 50 mol%, avg. MW 50000-75000, DL-lactide 85 mol%, and avg. MW 40000-75000, DL-lactide 50 mol%. The sonication method for particle formation produces polydisperse microspheres, shown in Figure 1.

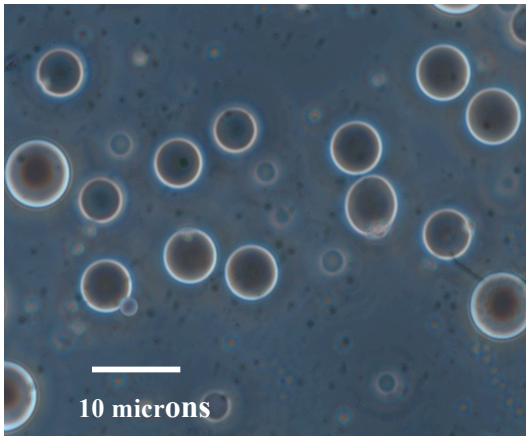

Figure 1. Light microscope image of emulsion microspheres prior to solvent evaporation. Water in oil emulsion (ultrasonic probe); poly(DL-lactide-co-glycolide), MW 5000-15000, DL-lactide 50 mol-%.

Vibrating orifice aerosol generators were used for test production for the PLGA based mixtures listed above. The method produced a narrow size distribution in the 4-5 micron size range and proved to be highly suitable for the solvents and small scale production. The use of a VOAG was ruled out due to a low likelihood this method could be used for large scale production (grams).

Due to instrumental limitations, VOAG particle formation methods are not capable of producing particles less than 1 micrometer in diameter or in large quantities as needed for future tests. Therefore an alternative method was tested. For scale-up and small particle (< 1 micrometer) syntheses we have employed a Sono-Tek ultrasonic atomizer, Model 8700-120. The 120 kHz nozzle produces droplets with a median size of 18 micrometers allowing for smaller particle production compared with either the VOAG (droplet size-25 micrometers) or ink jet (droplet size-30 micrometers). This technology necessitates sorting of the polydisperse product via an in-line four stage or eight stage cascade impactor. Particles of the previously described PLGA/acetone solution were collected using this methodology.

Inkjets were used to demonstrate a scalable and low cost method for microsphere production. Inkjets have the ability to tightly control droplet size and have been proven to be durable by consumers. These properties along with the ability to run multiple inkjets in a parallel system may prove to be ideal for the production of bio-safe microspheres. Print heads produce droplets in the range of ~10 to 90 pL. This size range is capable of producing dried particles in the target range needed for bio-surrogates.

In all cases except for the spheres produced with an ink jet, florophores were added and the resulting particles were tested with a variety of measurement methods including fluorescence and size. In limited cases the resulting particles were tested for charge and long term stability.

Fluorescence:

Overview:

A number of suitable lipophilic fluorophores have been identified and analyzed for their solubility and fluorescent properties. Dipicolinic acid, tyrosine and tryptophan were evaluated for use to simulate a *B. anthracis* emission spectrum.

Fluorescent measurements were made using Total Luminescence Spectroscopy (TLS) and LLNL'S Single Particle Mass Spectrometer (SPAMS) system. TLS provides an emission spectrum for multiple excitation wavelengths and thus yields detailed information of the fluorescent properties of a substance. A typical TLS spectrum is shown in figure 2.

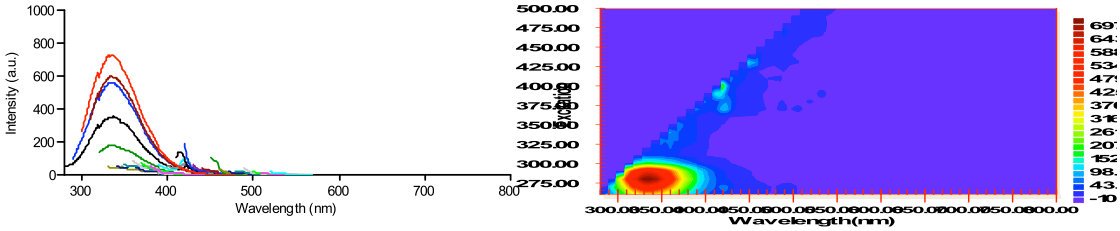

Figure 2. Typical TLS spectrum. On the left a single excitation wavelength with multiple intensities. On the right a 3-d plot of excitation vs. emission wavelength.

TLS Measurements of Baculovirus BV-55, Riboflavin and Ricin toxoid:

Several additional bio-threats and simulant materials were analyzed with TLS. These include AcNPV (baculovirus), acetylated riboflavin and ricin toxin. Baculovirus TLS is shown in Figure 3.

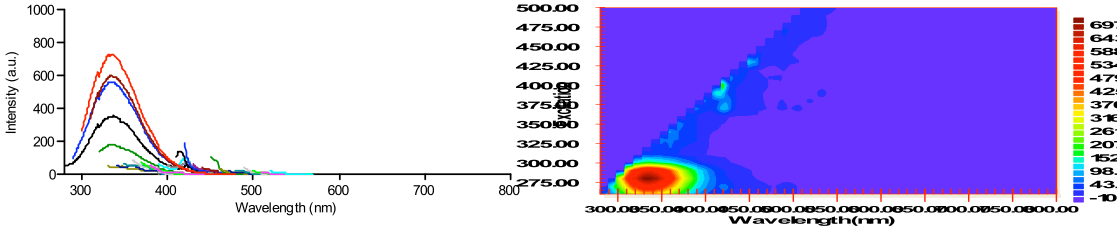

Figure 3. TLS analysis of purified, concentrated Baculovirus BV-55; excitation 260 nm; emission peak maxima 334 nm.

Acetylated riboflavin was successfully incorporated into the polymer microspheres at 10 wt% concentration using a SonoTek atomizer. Total luminescence spectral analysis

(TLS) of the doped microspheres revealed 2 peaks at excitation wavelengths of 265 and 370 nm and emission at 526 nm (Fig. 1). Riboflavin quantum yield is very high (0.30) making it a good candidate for loading into smaller particles, 0.5-1.0 mm, where strong emitters are required for detection. Scanning electron microscopy imaging of the particles is shown in Figure 4. Particles are spherical; dimpled or porous particles were not observed.

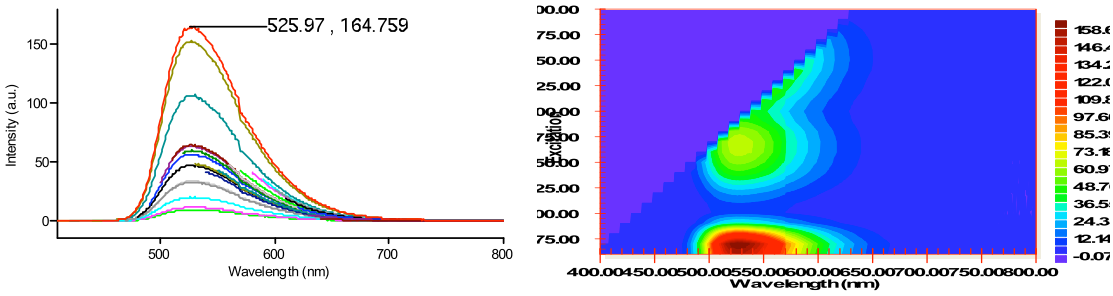

Figure 4. TLS analysis of acetylated riboflavin spheres; 3D contour map shows 2 peaks with excitation maxima of 265 and 370 nm and emission maxima of ~526 nm.

We obtained ricin toxin, extracted from *R. communis* beans, that has been chemically inactivated (BEI Resources, NR-4671). TLS analysis, to characterize fluorescent behavior, showed no unique features for discrimination. The observed fluorescence was similar to proteins with a large tryptophan peak dominating the spectrum. Filters were used to remove 2nd order effects. Ricin toxin TLS is shown in figure 5.

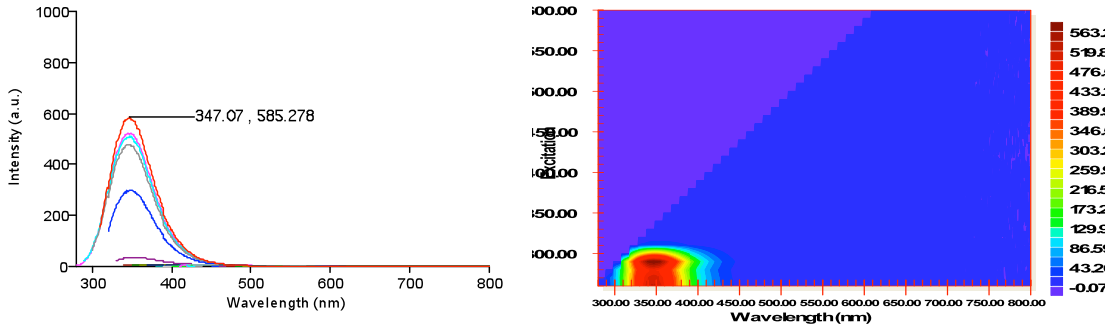

Figure 5. Total luminescence analysis of ricin toxoid. A large tryptophan peak at 347 nm was the only peak observed after subtraction of background.

TLS Measurements on PLGA/Poly-Tryptophan and *B Anthracis*:

An effort was made to simulate the TLS for B anthracis with PLGA and tryptophan. The results are shown below. Total luminesence spectroscopy was performed on both emulsion-PLGA/tryptophan and the VOAG-PLGA/poly-tryptophan microspheres. The resulting emission matrix was compared to that for *B. anthracis*. Figure 6 shows a comparison of the TLS spectra. The bottom frame shows the TLS spectra for *B. anthracis stern* spores. This spectrum was used as a target for microsphere spectral features. In the top frame a TLS is shown for the emulsion PLGA/tryptophan spheres. It is important to note that the area with the highest signal in Figure 1a is slightly shifted to higher wavelengths than the spectra for *B. anthracis*. This shift is on the order of 50 nm. In Figure 1b a TLS spectrum is shown for VOAG produced poly-tryptophan microspheres. The use of the poly-tryptophan reduces the spectal maxima shift to ~25 nm. Additional fluorescent measurements were collected with the single particle aerosol mass spectrometer. Although no quantitative measurements were made it was found that the biosafe microspheres had fluorescent qualities that triggered the system to collect mass spectra (they were determined to be biological like by the automatic detection system).

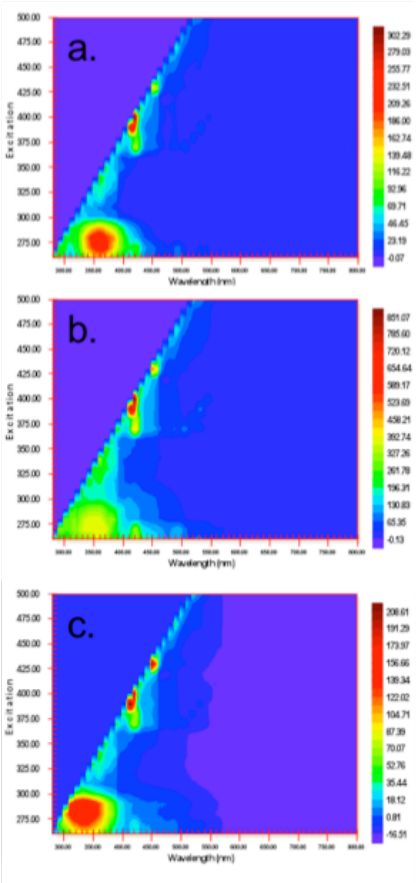

Figure 6. Total lumensence spectra. a) Emulsion-PLGA/tryptophan microspheres. b) VOAG-PLGA/polytryptophan microspheres c) *B. Anthracis Ames* spores

LLNL'S SPAMS Fluorescent Detection:

LLNL's SPAMS system was developed with fluorescent prescreening for mass spec identification of bio-threat agents. The SPAMS system with dual UV-LIF excitation wavelengths of 266 and 355 nm, two emission bands, a charge detection stage and multi-laser tracking for aerodynamic particle sizing was challenge-tested with tryptophan-doped microspheres. If fluorescence is detected in either or both emission bands and if a particle falls within the size range of interest, the particle is identified as biological or positive. Under normal operation a positive identification triggers a desorption/ionization laser to ablate the particle for mass spectral analysis and subsequent biological identification. In these tests we only employed the fluorescent prescreening and size measurement and charge detection. SPAMS fluorescence data is shown in figure 7. It is important to note that the SPAMS florescence measures single particles in a dual band. The separation into short and long emissions for both excitation wavelengths is ~400 nm.

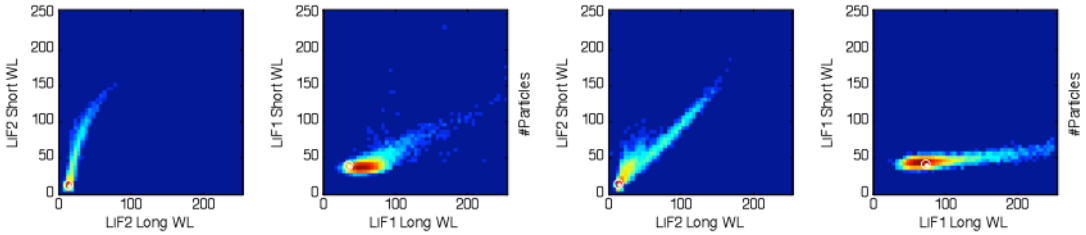

Figure 7. From left to Right: µ-spheres 266 emission spectrum, µ-spheres 355 emission spectrum, *B. Anthracis* 266 emission spectrum, *B. Anthracis* 355 emission spectrum.

The variations in µ-sphere and *B.* anthracis spectra are attributed to the variation in size. The SPAMS system was able to identify the µ-sphere particles as biological like.

Particle Charge Determination:

Principal of Operation:

Particle charge influences the transport properties of aerosols. Reproducing the charge of a bio-threat allows for better transport simulation and model validation. Particle charge was measured with the charge detector recently developed by the Single Particle Aerosol Mass Spectrometry Group at LLNL. A single particle enters a conductive tube and induces a charge on the tube. The mirror image charge is amplified and recorded. In order to calibrate the charge detector a small electrical pulse is injected into the tube through a capacitor. A diagram outlining the charge detection is shown in figure 8.

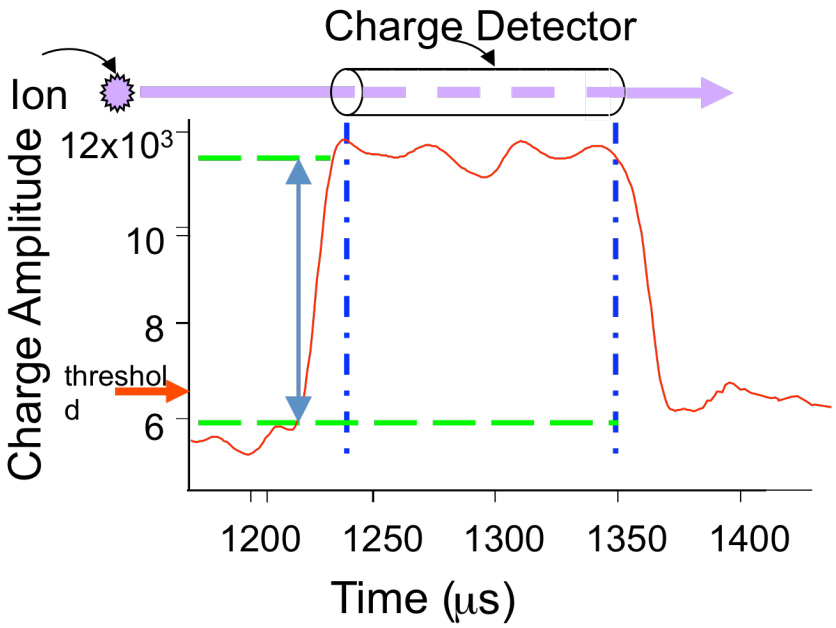

Figure 8. Principal of aerosol charge detection. Charged particles induce a charge on the detection tube and the resulting signal is recorded for each particle**.**

Charge Measuremtns of *B. Anthracis, Yersina* and µ-spheres:

Histograms were produced of the single particle charge measurements for bio-safe micro-spheres, *B. anthracis* and *Yersinia.* Charge histograms are shown in figure 9. The figure clearly shows the slightly wider charge distribution for the engineered micro-spheres compared to the simulated threat agents. The small gap in recorded charge near the zero charge line is an artifact of the amplifiers and digitizers used in the current apparatus and should not be interpreted to mean that there are no particles with zero charge. The wider charge distribution for PLGA particles is attributed to the larger size range 4-5 µm for PLGA 1-3 µm for *B. anthracis* and *Yersinia*.

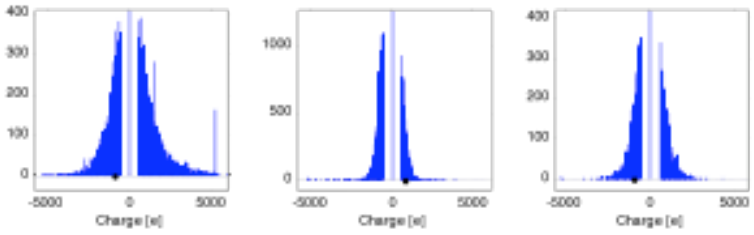

Figure 9. Charge histograms. Left: PLGA microspheres. Middle: *B. anthracis*. Right: *Yersinia*

The wider charge distribution for PLGA particles is attributed to the larger size range 4-5 μm for PLGA 1-3 μm for *B. anthracis* and *Yersinia*. A second possibility of the wider distribution is the age of the particles tested. The μ-spheres were produced more recently than the bio-agents.

Physical Properties:

Size Determination:

In order to properly mimic the transport and inhalation properties of bio-threats size must be property reproduced. Several commercially available techniques are available for aerosol size measurement in the 1-10 μm size range. The experiments employed an Aerosol Particle Sizer (TSI Inc.), optical microscopy, scanning electron microscopy, and LLNL's Single Particle Aerosol Mass Spectrometer (SPAMS). All of the size determination methods are capable of measuring the appropriate size range and have unique advantages. The APS and SPAMS are very rapid methods for determining the aerodynamic size profile for a large number of particles. Both optical and SEM size determination determine the physical size of the particles with the added benefit of determining the shape of the particle.

The two methods of producing microspheres had very different size distributions. As expected the emulsion method produced particles ranging from 0.7- 4.7 μm. The VOAG method produced a much narrower size distribution of 4-5 μm. Figure 10 shows SEM images of microspheres produced by emulsion and VOAG methods. It was also determined that particles produced by the Sono-Tek aerosol generator had a poly-dispersed size distribution.

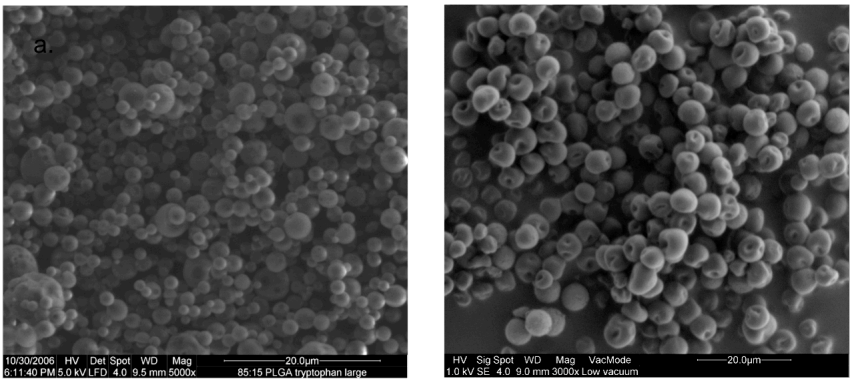

Figure 10. SEM images of microsperes. Left: Emulsion-synthesized PLGA/tryptophan microspheres; size range 0.7– 4.7 mm. Right: VOAG/solvent evaporation-synthesized PLGA/poly-tryptophan microspheres; size

Inkjet print heads were demonstrated to produce a narrow size distribution, figure 11. An HP (model # Deskjet D2545, HP 60 cartridge) inkjet has been modified by drilling a hole into the bottom of the printer to allow for the collection of aerosols. This simple approach utilizes all of the software and hardware that has been optimized for the consumer market. Figure 11 shows the results from a 10% w/v solution of Glucono-delta-lactone in water. The particles were passed through a drier and the dried particles measured with an APS. There is a tight size distribution in the 2-3 micron size range, 61% of the aerosol mass is in this region. This is an extremely low cost solution for the production of small amounts of aerosols.

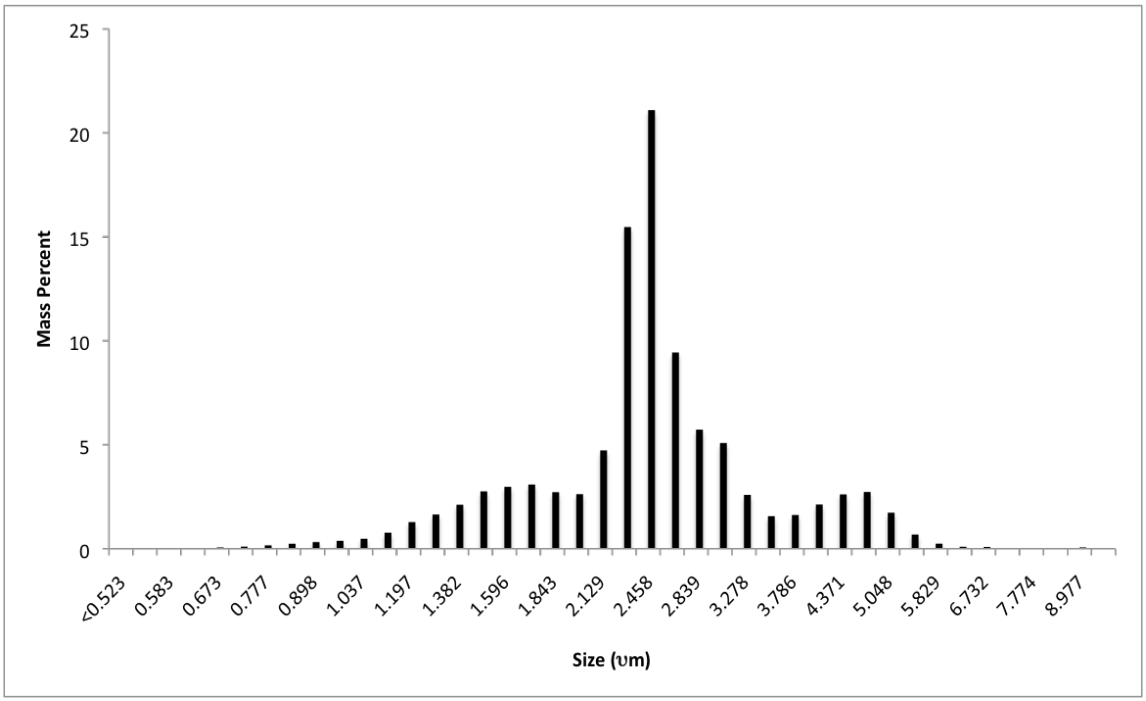

Figure 11. APS size distribution of 10% w/v solution of Glucono-delta-lactone in H20

Hydrophobicity:

Hydrophobicity measurements were completed using Rose Bengal partitioning, a technique where the microorganisms/microspheres are exposed to the hydrophobic-binding stain for a determined period of time, centrifuged, and the supernatant analyzed at OD_{542} to measure the decrease in absorbance due to stain adhesion to the particle surfaces. Surface hydrophobicity was determined for *Bacillus anthracis* Sterne endospores and microspheres. The partitioning quotient (PQ) is defined as the following:

$$\frac{\text{amount of Rose Bengal adsorbed to the surface}}{\text{amount of Rose Bengal is the dispersing medium}}$$

By varying the concentrations of spores or particles in suspension, a linear relationship between PQ and total surface area is obtained, which is a measure of surface hydrophobicity (Fig. 12). The *Bacillus anthracis* Sterne spores exhibit a strong affinity for Rose Bengal, in agreement with the hydrophobic nature of *Bacillus* spores. Partioning quotients for the 80:20 PLGA spheres is in agreement with published values for PLGA microspheres (Walter et al., 2001). The 80:20 PLGA is a relatively hydrophobic co-polymer due to the high percentage of lactide monomer. It may be possible to further modify surface hydrophobicity by incorporating hydrophobic groups on the microsphere surface.

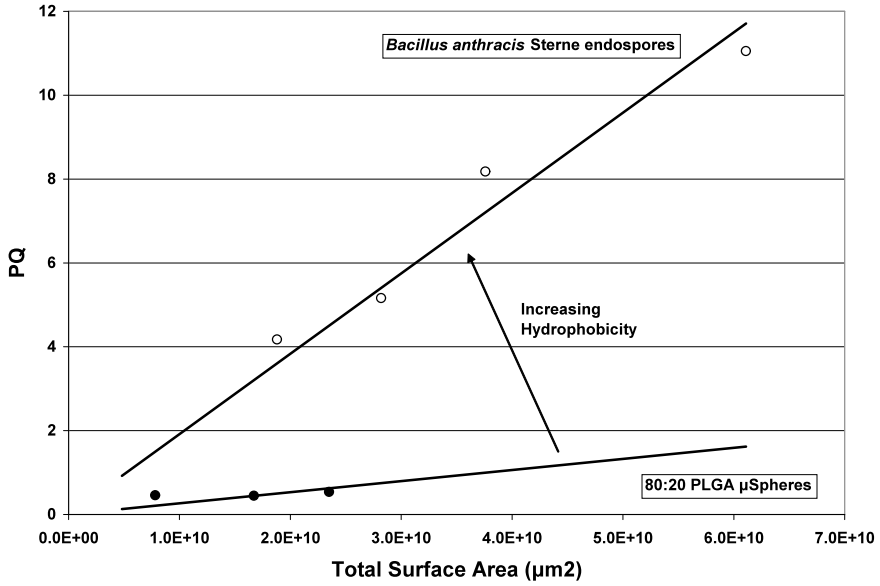

Figure 12. Partitioning coefficient (PQ) of Rose Bengal at increasing surface area for 80:20 PLGA microspheres and *Bacillus anthracis* Sterne endospores.

Density:

An SEM equipped with a focused ion beam was used to image microspheres (80:20 PLGA polymer, Polysciences, Inc with 10% acetylated riboflavin fluorophore). An area was selected for FIB x-sectioning and the FIB was used to deposit a protective layer of Pt over the microspheres. The FIB was setup to perform a Slice & View operation. The slice pitch can be adjusted depending on the volume of area to be sectioned. The slice pitch was set at approximately 50nm/slice. An SEM image was taken after every slice, with a relative angle to the FIB x-sectioning set at 52 degrees. The SEM images or image stacks were downloaded to animation software to create a movie at the completion of the Slice & View operation (Fig. 13). This approach clearly shows interior cavities in the microspheres. The large microspheres in the image were completely hollow, whereas a smaller sphere contained multiple cavities, but one small microsphere was completely solid. These results are consistent with the Pan et. al work (appendix A).

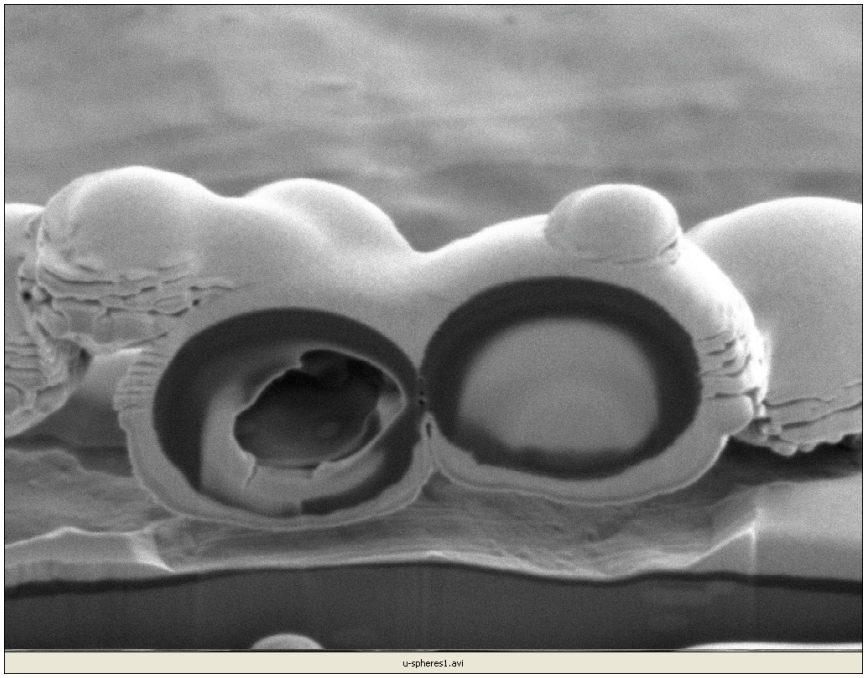

Figure 13. Still image from a movie of the sequential Slice & View operation used to image cross-sections of the 80:20 PLGA microspheres

Particle Stability:

Particle stability or shelf life is a critical property for field testing. Without the ability to produce and store for a reasonable period of time it would be imposible to produce simulants to be used in the field. Stability testing of acetylated-riboflavin microspheres subjected to two temperature and two relative humidity treatments were completed. Aliquots were removed from the test chambers and analyzed at three timepoints. SEM stubs, placed in each treatment condition, contained registration marks to allow for repeated imaging of selected areas.

Experiments were conducted under varying aging conditions including changes in relative humidity RH. Aliquots treated at 7% RH showed no morphological effects after 26 days of exposure. The results are shown in figure 14.

Electron beam damage was observed in aliquots treated at either 37^{o}C or 75% RH. Damage was not evident during T_0 analysis rather after treatment and re-imaging in the same location. (Images of these particles were included in the January report.) For subsequent SEM analysis of these treatments, images were not taken in the same locations as had been previously recorded.

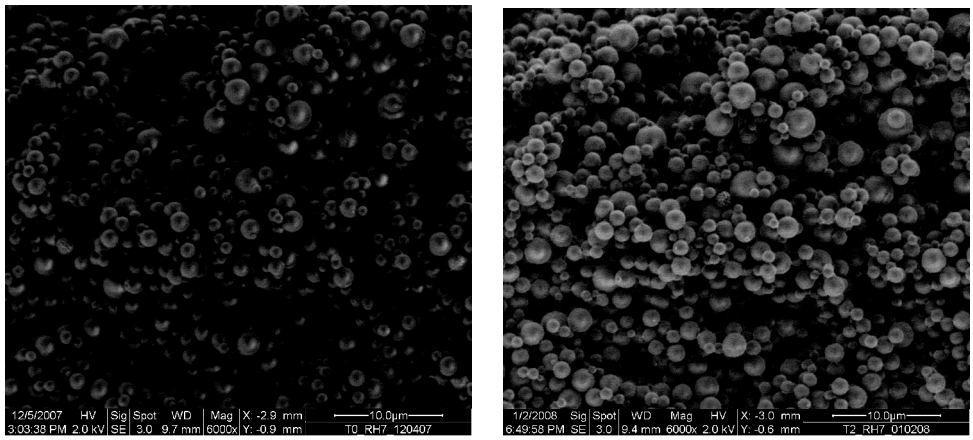

a. b.

Figure 14. Microspheres treated at 7% RH for 0 (a) and 23 days (b) show no morphological changes. Images were taken at the same location.

Beam damage may be indicative of changes in the microspheres after exposure to wet and hot conditions – conditions that the polymer is most susceptible to and thus might have the greatest impact on stability (PLGA co-polymers are hygroscopic and have fairly low glass transition temperatures). The particles may have been "sensitized" to beam damage after these more extreme treatments.

The figures that follow are images of aliquots treated at 75% RH for 29 days (Figure 15), 22^{o}C for 26 days (Figure 16), and 37^{o}C for 26 days (Figure 17). The treatments did not appear to impact particle morphology over these time periods.

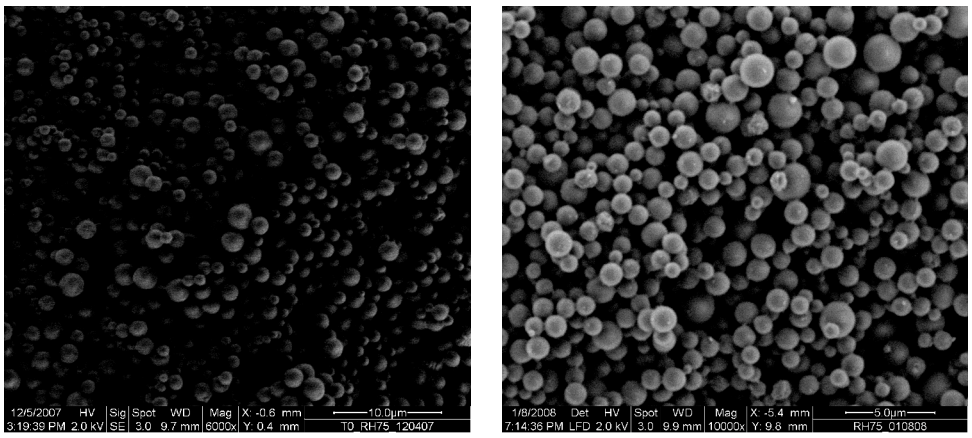

a. b.

Figure 15. Microspheres treated at 75% RH for 0 (a) and 29 days (b). Images were taken in different locations to avoid beam damage effects. Particles appear intact and robust after 29 days at elevated relative humidity.

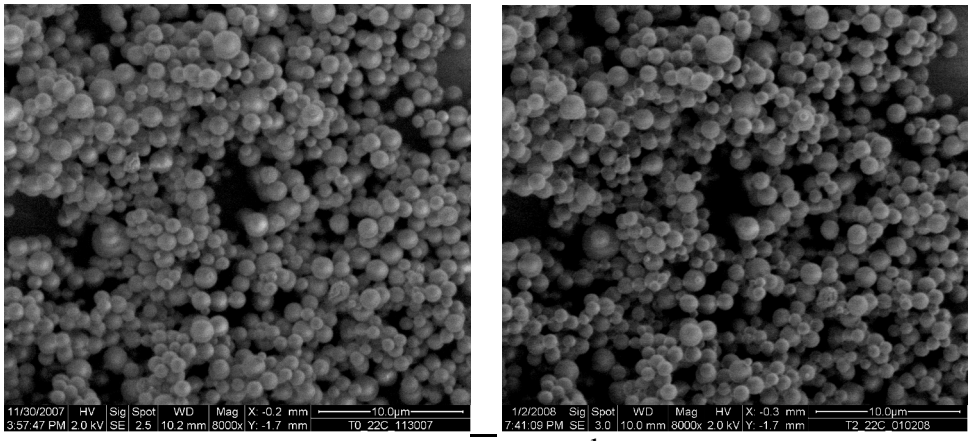

a. b.

Figure 16. Microspheres incubated at 22°C for 0 (a) and 26 (b) days and imaged in the same location appeared identical with no changes in morphology.

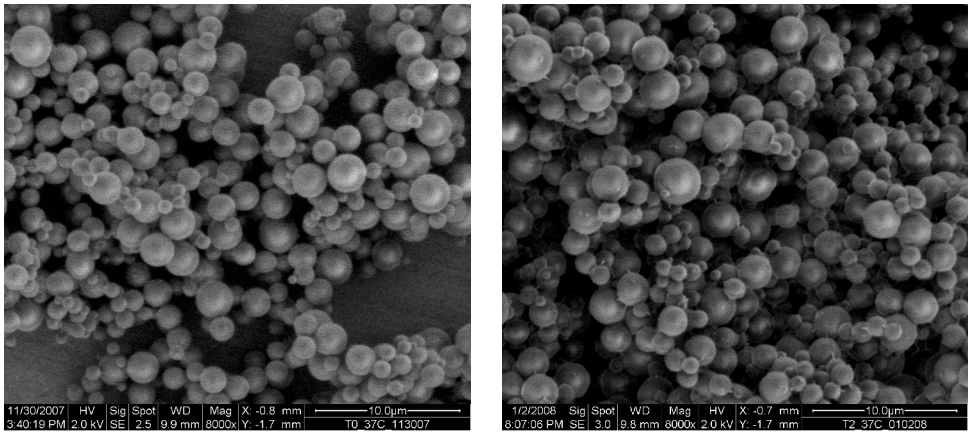

a. b.

Figure 17. Microspheres incubated at 37°C for 0 (a) and 26 (b) days and imaged in areas not previously exposed to the electron beam appear robust with no morphological changes.

CONCLUSIONS AND FUTURE WORK:

The production of bio-safe micro-spheres with a VOAG, Sono-Tek and emulsion techniques were demonstrated to reproduce many of the desired characteristics of a simulated threat agent. By using tryptophan and poly-tryptophan as the only fluorophore a close match to the TLS of *B. anthracis* was achieved. Fine-tuning of the fluorescent properties with additional chemicals should prove the ability to match most if not all threat agents.

The tested methods show the ability to produce particles in a size range that would be applicable for threat agent simulants. However, with poly-dispersed methods such as the emulsion technique, and Sono-Tek aerosol generator costly and time consuming size

sorting would be required. The VOAG has the capability of producing a mono-dispersed particle type but has significant drawbacks in the ability to mass-produce particles at a low cost. Commercial ink jet print heads allow for a tight size distribution in the desired 1-3 micron size range at a very low cost and with production scalability.

In addition to the work shown in this report the research has given insight into some future research aspects. It has been proposed that by using food based simulant particles a safe inhalable simulant can be produced. Currently this is being explored using gluco-delta-lactone FDA approved food products. It is intended that the new research area will also incorporate DNA into the particles for use in the Pentagon Shield program. Appendix C includes a letter of support from the Pentagon Force Protection Agency.

Appendix A (Pan, Pinnick final report)

Particle-fluorescence spectrometer (PFS) measurements of PLGA test aerosol particles

Yong-Le Pan[a], Ronald G. Pinnick[b], Steven C. Hill[b], Richard K. Chang[a]

[a]Department of Applied Physics, Yale University, 15 Prospect St., New Haven, CT 06520, USA

[b]US Army Research Laboratory, 2800 Powder Mill Road, Adelphi, MD 20783, USA

Abstract

Measurements of single-particle laser-induced-fluorescence (LIF) of various PLGA test particles made with the dual-excitation wavelength Yale/ARL Particle-fluorescence spectrometer (PFS) are reported. The PFS can: 1) measure fluorescence spectra of bacterial particles having light-scattering sizes as small as 1 μm, and 2) measure each particle's elastic scattering which can be used to estimate particle size. Smaller PLGA test particles are more uniformly loaded with tryptophan than larger ones. Both riboflavin-doped and retinol-doped PLGA particles appear more uniformly loaded than tryptophan-doped PLGA particles.

1. The Particle Fluorescence Spectrometer

Figure 1 illustrates the PFS detection system.

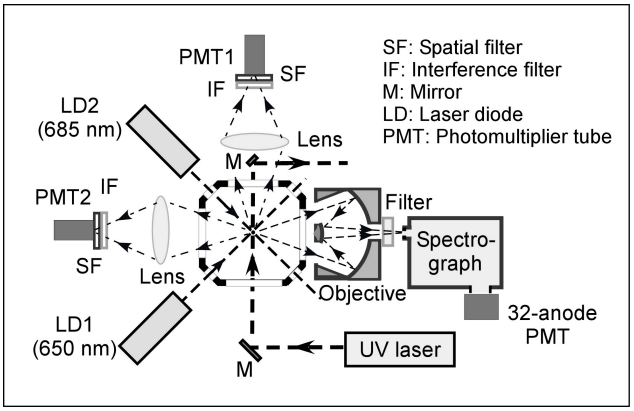

Fig. 1. Schematic of the Particle Fluorescence Spectrometer. Aerosol is drawn into the inlet where the particles having sizes between 1 and 10 μm are drawn into a 2" cubic optical cell through a double aerodynamic focusing-nozzle forming a laminar (inner) aerosol jet surrounded by a clean air sheath flow. Single particles within the aerosol jet are probed on-the-fly as they flow through the cell with two pulsed UV lasers (only one shown here), which excites fluorophors within the particles. The fluorescence emission is collected by a reflective objective, focused onto a slit, dispersed by a curved grating, and

detected with a 32-anode PMT. This arrangement permits rapid measurement of single-particle fluorescence spectra, with aerosol sample rates of the order of 1 liter per minute for 1-10 micron particles.

2. Tests of the PFS System and its Calibration

The PFS efficiently excites, collects, disperses, and senses fluorescence emission from single particles illuminated by each of two sequential UV laser pulses. We calibrated and tested the PFS aerosol sample flow rate, sensitivity, and fluorescence spectral response by generating test particles from insoluble particles such as dye-impregnated polystyrene latex micro-spheres and *Bacillus subtilis* spores; we also dissolved tryptophan in water, aerosolized the resulting solution, and dried the particles for measurement. Particles of these different samples were generated with either a Royco generator or an Ink Jet Aerosol Generator (IJAG).

2.1 *Fluorescence and Elastic Scattering Measurements of Uniformly Sized Fluorescent Polystyrene Beads*

To ascertain the amount of variation in scattering and fluorescence that are intrinsic to the PFS, we tested the PFS with relatively uniformly sized, nominal 2-μm diameter, polystyrene latex beads that were doped with a blue dye. The coefficient of variation (CV) in diameter for these particles is given by the manufacturer to be "less than" 5%, and so the particle's CV in cross section is about 10%, and the CV in volume is about 16%. If the dye is uniformly distributed within the microspheres, the fluorescence should be proportional to d^x where x is some number between 2 and 3. The beads are about 6 wavelengths in diameter with relatively large refractive index. We cannot calculate what x is because we do not know the absorption cross section of the dye molecules or the concentration of dye.

A scatter-plot of the fluorescence vs. elastic scattering measured with the PFS for these 2-μm diameter spheres is illustrated in Fig. 2. Histograms of the elastic scattering and fluorescence are also shown, along with best fit Gaussian curves for the histograms. For the elastic scattering the CV measured is 16.5%. The total scattering by the sphere increases approximately as the cross section. However, the scattering in the 60 to 120 degree range measured by the PFS may increase more slowly than cross section because as the sphere size increases the fraction of the light that is forward-scattered tends to increase. There is a positive skew (0.353) which would be expected for particles that have a Gaussian distribution in diameter, but where the scattering increases faster than diameter, e.g., as diameter squared. For the fluorescence histogram in Fig. 2, the CV measured is only 10%. If the fluorescence were distributed evenly throughout the sphere, and if the CV for the size were 5%, not "less than" 5%, then the CV would be expected to be between 10% (x=2) and 16% (x=3). The measurement of a CV at the very low end of this range suggests that the PFS contributes a relatively small increase to the CV of the fluorescence. Again the skew is positive, which is not surprising.

A best-fit line for the scatter plot of the fluorescence vs elastic scattering is also indicated in Fig. 2. The positive slope to this line could be because: a) some spheres are in a part of the beam where the intensity is greater, and/or, b) the larger spheres both scatter more and have more fluorescence.

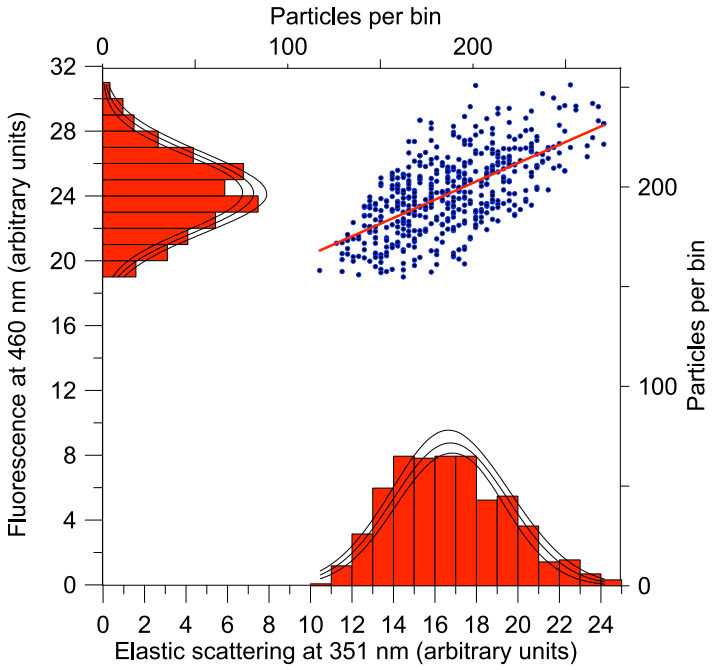

Figure 2. Single-particle laser-induced fluorescence vs. elastic scattering measured with the PFS for blue-dye doped fluorescent polystyrene beads with nominal diameter 2-μm (coefficient of variation is "less than" 5%). Also shown is the best fit line. Histograms for both LIF and elastic scattering measurements are shown.

The fact that the fluorescence tends to increase with elastic scattering suggests that the CV in the ratio of fluorescence to elastic scattering should be less than the CV of the elastic scattering. The CV for the ratio of the fluorescence to elastic scattering is 12%.

2.2 *Fluorescence Spectra of nominal 1.36- μm Bacterial Particles*

Bacillus subtilis vegetative cells were aerosolized and their elastic scattering and fluorescence spectra were measured with the PFS. Figure 3 shows a scatter-plot of the fluorescence vs. elastic scattering, as well as histograms of the elastic scattering and fluorescence, and a best fit Gaussian curves for the histograms.

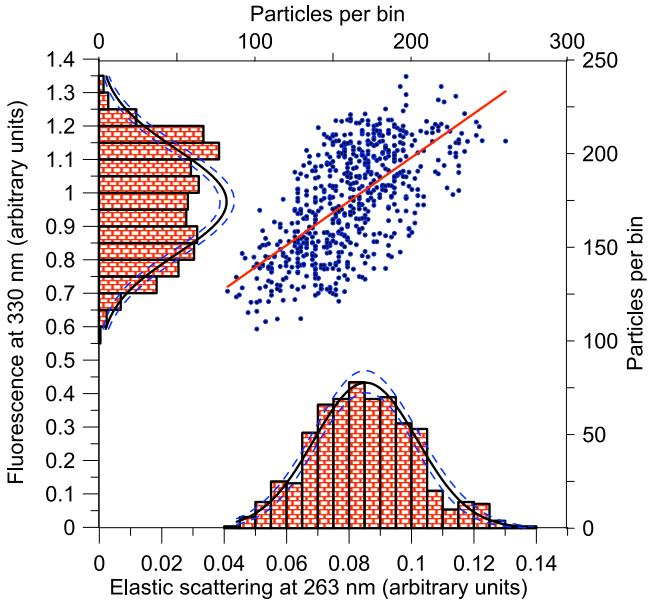

Figure 3. Single-particle laser-induced fluorescence vs. elastic scattering measured with the PFS for B. subtilis spores with nominal diameter 1.36-μm. Also shown is the best fit line. The lower histogram is of the single-particle laser-induced elastic scattering (CV=19%). The upper histogram of the fluorescence (CV=16%).

Figure 4 shows the fluorescence spectra of some of the 1.36-μm- diameter *B. subtilis* spores included in the analysis of Fig. 3. These indicate the uniformity of the fluorescence signal from bacterial spores with good signal to noise ratio. The broad fluorescence peak (at 340 nm) derives mainly from tryptophan; the tail from 400 to 500 nm is may be attributable to fluorescent compounds of the growth material in which the bacteria were grown, but may also have contributions from reduced nicotinamide compounds such as nicotinamide adenine dinucleotides.

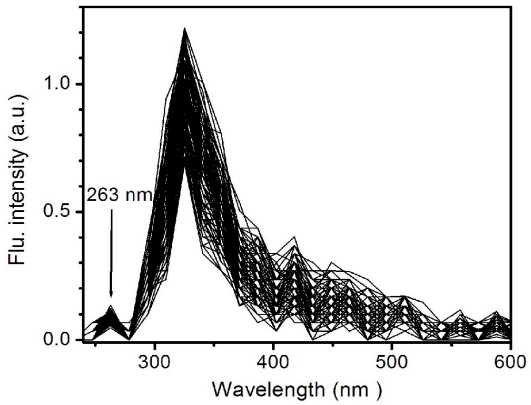

Figure 4. Normalized PFS fluorescence spectra of 300 *Bacillus subtilis* particles having nominal 1.36-μm (light-scattering) diameter excited by single-shot (263-nm wavelength) laser pulses. The peak at 263 nm is the elastic scattering of the pulsed 263-nm laser beam from the particles leaking through the long-pass filter, which is used for estimating particle size.

2.3 *Elastic Scattering/Size calibration of the Particle Fluorescence Spectrometer using Uniformly Sized Polystyrene Latex particles*

To estimate particle size from elastic scattering in the PFS system, we aerosolized polystyrene latex micro-spheres (Duke Scientific Corp.) having diameters of 1, 2, 3, and 4.3 μm and drew them through the system. The particles were suspended in water and aerosolized using a Royco Aerosol Generator. The (elastic scattering) response of the PFS to the latex micro-spheres is summarized in Fig 5. We note that PFS response is approximately proportional to particle area.

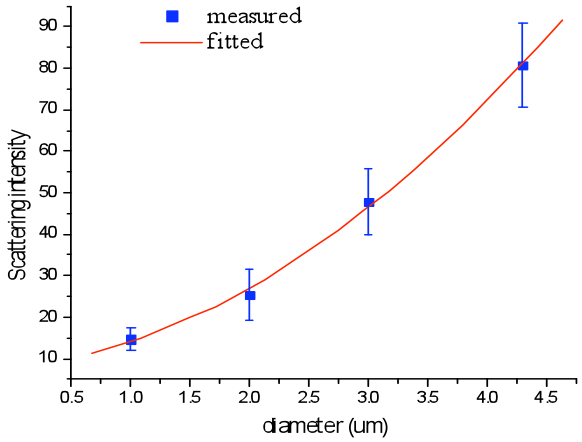

Fig 5. PFS (elastic scattering) response to uniform polystyrene latex microspheres for 351nm excitation. Microspheres are from Duke Scientific Corp. with nominal sizes at 1, 2, 3, 4.3 -μm with 5% coefficient of variation.

3. *Dispersal of PLGA test particles.*

PLGA test samples were dispersed in dry form (no liquid aerosolization process). Samples of scanning electron micrographs of some PLGA test samples impregnated with tryptophan are shown in Figs. 6 below.

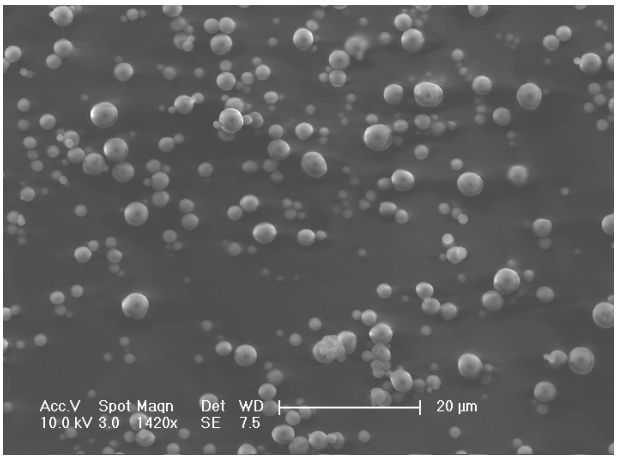

PLGA_tryp_stage 3-low resolution

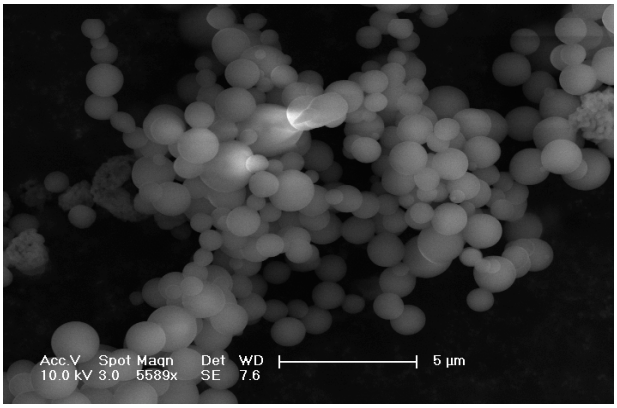

PLGA_tryp_stag4-low resolution

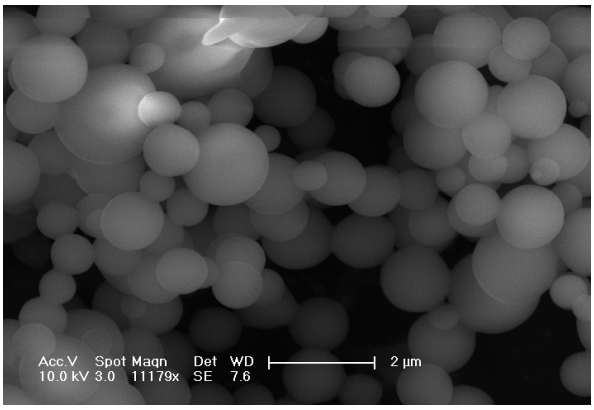

PLGA_tryp_stag4-high resolution

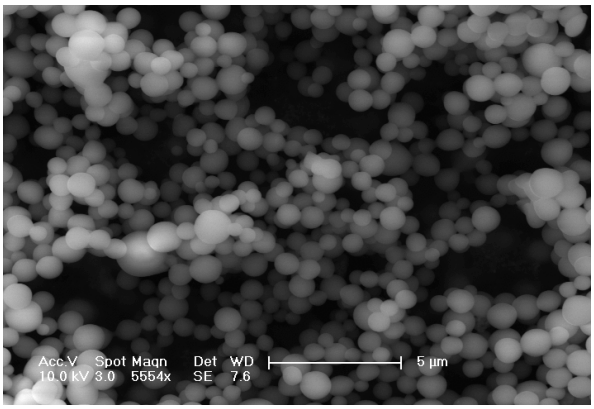

PLGA_tryp_stag5-low resolution

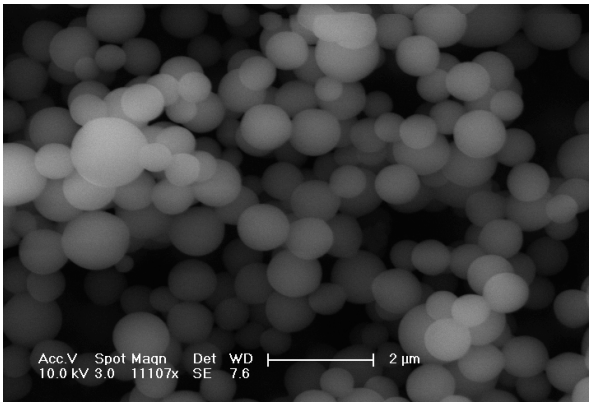

PLGA_tryp_stag5-high resolution

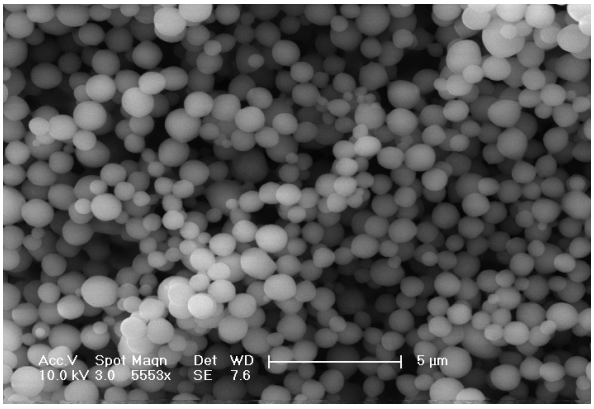

PLGA_tryp_stag6-low resolution

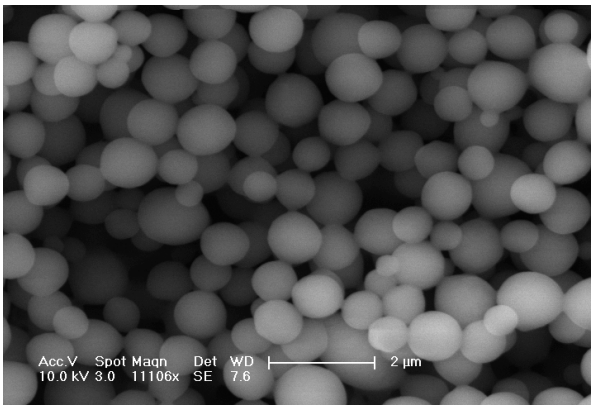

PLGA_tryp_stag6-high resolution

Fig. 6. SEM images of some PLGA-tryptophan loaded samples

4. *Measurement of tryptophan-doped PLGA test samples with the PFS*

The dry-dispersed PLGA test samples were fed to the inlet of the PFS and fluorescence spectra from single particles excited sequentially with two pulsed UV lasers were measured. Fluorescence excited at 263 nm was measured over the 280-700 nm spectral range and fluorescence excited at 351 nm was measured from 380-700 nm. Leakage from the 351 nm or 263 nm elactic scattering signal was used to estimate particle size. Typical fluorescence spectra of PLGA test particles excited at 263 nm are shown in Fig. 7 below.

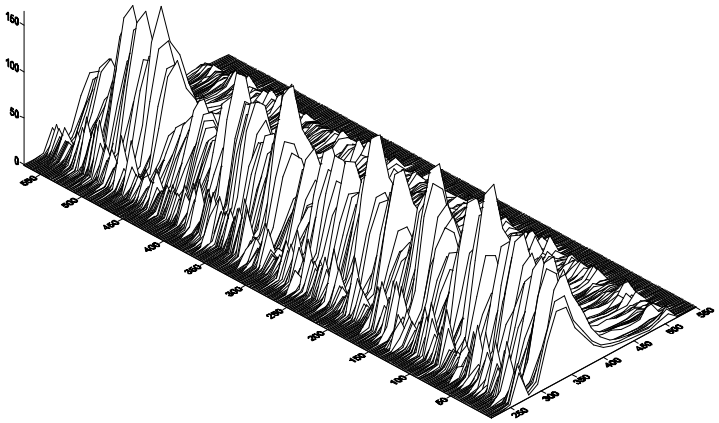

Fig. 7. Fluorescence spectra (3-D landscape view) of PLGA particles impregnated with tryptophan and excited at 263 nm wavelength (PLGA_tryp_stag6_80-20_082807)

A better indication of the variability of the spectra for the same data is evident in Fig 8.

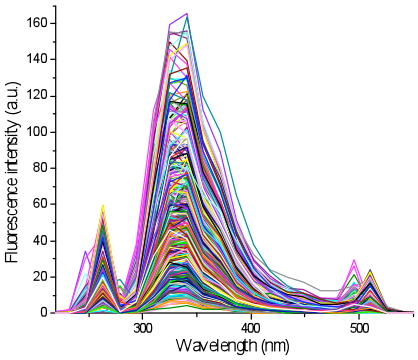

Fig. 8. Fluorescence spectra (2-D) of PLGA particles impregnated with tryptophan and excited at 263 nm wavelength (PLGA_tryp_stag6_80-20_082807)

For PLGA test particles loaded with significantly less tryptophan, a second peak occurs in the fluorescence spectra, as is evident in Fig 9.

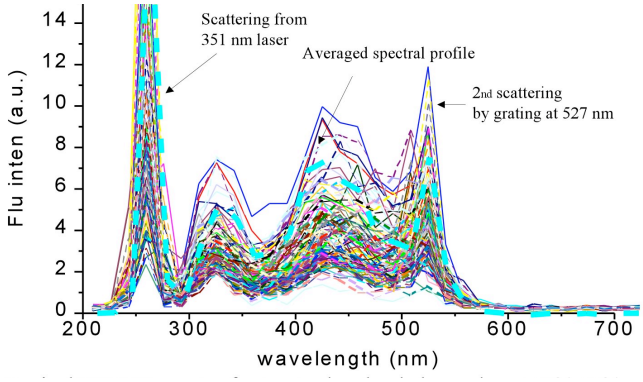

Fig 9. Typical UV-LIF spectra (excited at 263 nm) for PLGA particles loaded with tryptophan (sample PLGA_tryp_stage 4_50-50_082807). The average spectral profile is shown by the light blue dashed curve.

In order to investigate the size dependence of the PLGA particle fluorescence emission, we determined from our measurements the integrated fluorescence emission for each particle (from 290 nm through 510 nm) and approximate particle size (determined from the elastic scattering measurement using our calibration with polystyrene latex particles shown in Fig 5 above). The results are summarized in Figs 10 through Figs 15 for the various PLGA preparations. Also shown in these figures is the ratio of integrated fluorescence to particle diameter and to particle diameter squared.

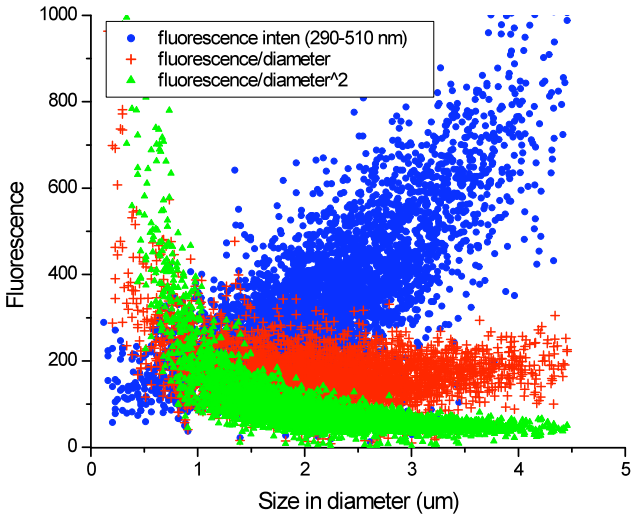

Fig. 10 Sample loaded with tryptophan: PLGA_tryp_stage3_80-20_082807

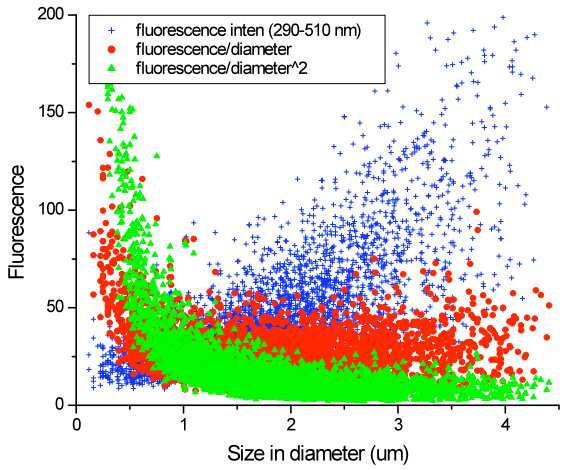

Fig. 11 Sample loaded with tryptophan: PLGA_tryp_stag4_50-50_082807

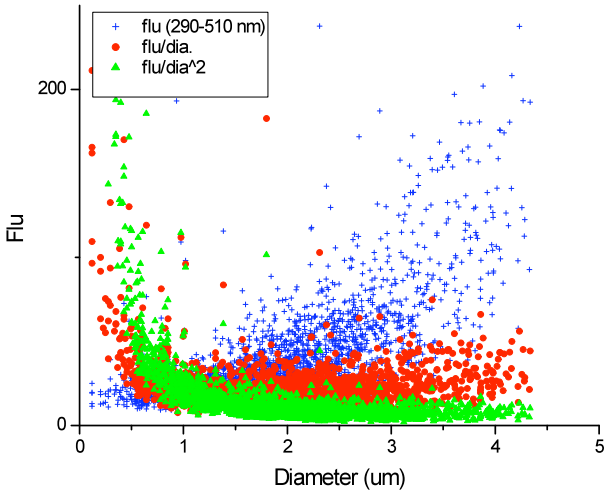

Fig. 12 Sample loaded with tryptophan: PLGA_tryp_stag4_80-20_082807

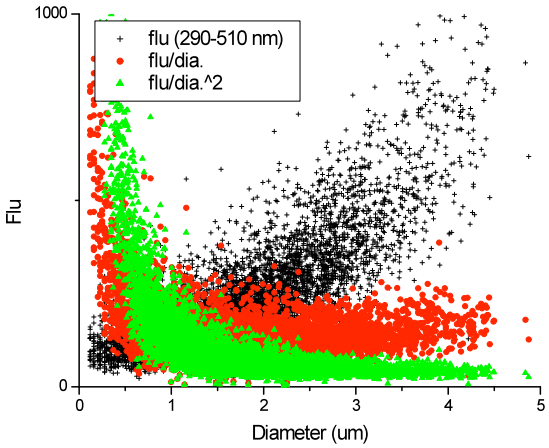

Fig. 13 Sample loaded with tryptophan: PLGA_tryp_stag5_50-50_082807

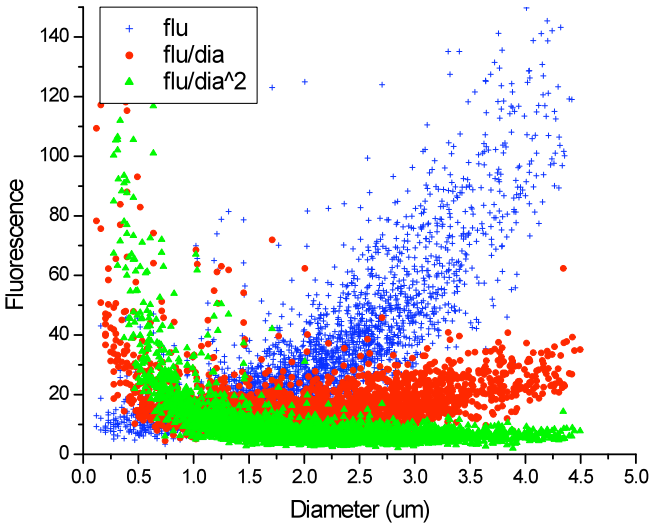

Fig. 14 Sample loaded with tryptophan: PLGA_tryp_stag5_80-20_082807

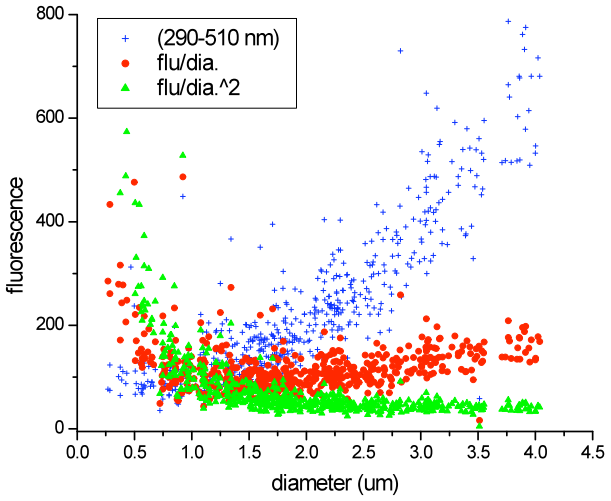

Fig. 15 Sample loaded with tryptophan: PLGA_tryp_stag6_80-20_082807

5. *Measurement of Riboflavin-doped PLGA test samples with the PFS*

The riboflavin-doped PLGA test particles were also dispersed dry. Typical elastic fluorescence spectra excited by a pulsed 351 nm laser are shown in Fig 16.

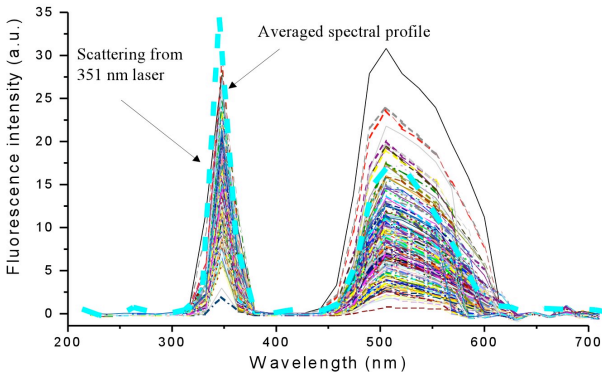

Fig.16 Typical UV-LIF excited by a 351 nm laser (with averaged profile) for "PLGA_RBF_stage 3-4-5_80-20"-microsphere particles loaded with acetylated-riboflavin.

The corresponding size distribution of the riboflavin-doped PLGA test particles, as measured with the PFS system are shown if Fig.17. Mean diameter is about 3 μm.

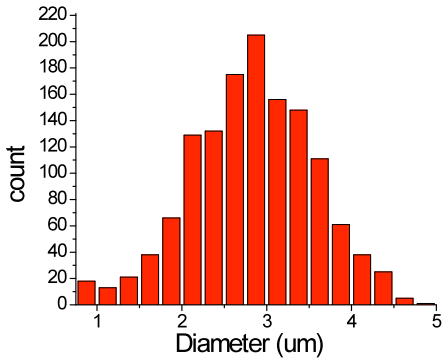

Fig. 17. Size distribution of riboflavin-doped PLGA test particles (sample PLGA_RBF_stage 3-4-5_80-20b)

The corresponding fluorescence-scattering size scat-plot is shown in Fig. 18, as well as the ratio of integrated fluorescence to particle diameter and to particle diameter squared.

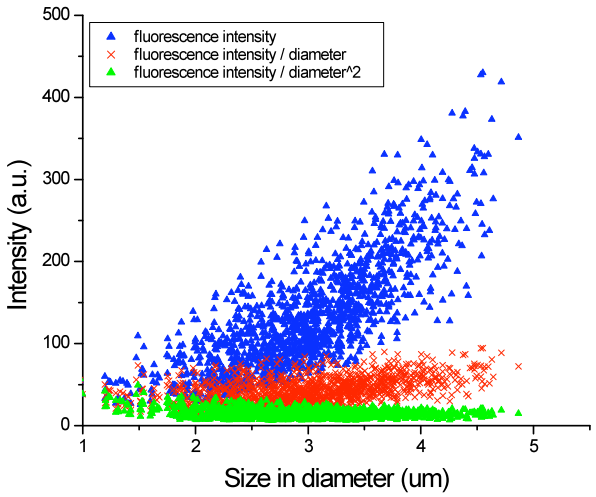

Fig. 18 Fluorescence, fluorescence/diameter, and fluorescence/diameter^2 varies with particle size for smaple loaded with riboflavin: PLGA_RBF_stag3-4-5_80-20b

6. *Measurement of Retinol-doped PLGA test samples with the PFS*

Again the retinol-doped PLGA test particles were also dispersed dry. Typical elastic fluorescence spectra excited by a pulsed 351 nm laser are shown in Fig 19. As is evident from the figure, the retinol-doped test particles have weak fluorescence compared to tryptophan- or riboflavin-doped particles.

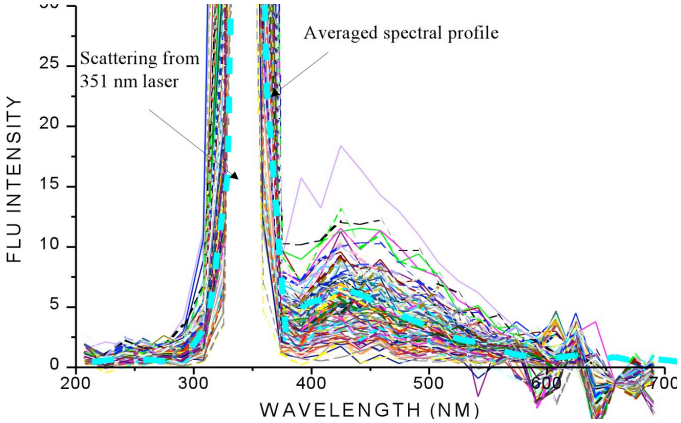

Fig. 19 Typical UV-LIF excited by a 351 nm laser (with averaged profile) for "PLGA_retinol_stag4_80-20".

The corresponding size distribution of the retinol-doped PLGA test particles, as measured with the PFS system are shown if Fig. 20. Mean diameter is about 4 μm. The corresponding fluorescence-scattering size scat-plot is shown in Fig. 21, as well as the ratio of integrated fluorescence to particle diameter and to particle diameter squared.

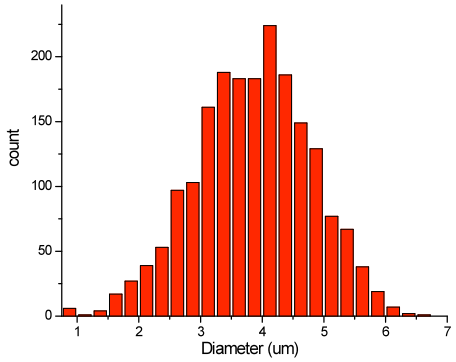

Fig. 20 Size distribution of retinol-doped PLGA test particles (PLGA_retinol_stag4_80-20b)

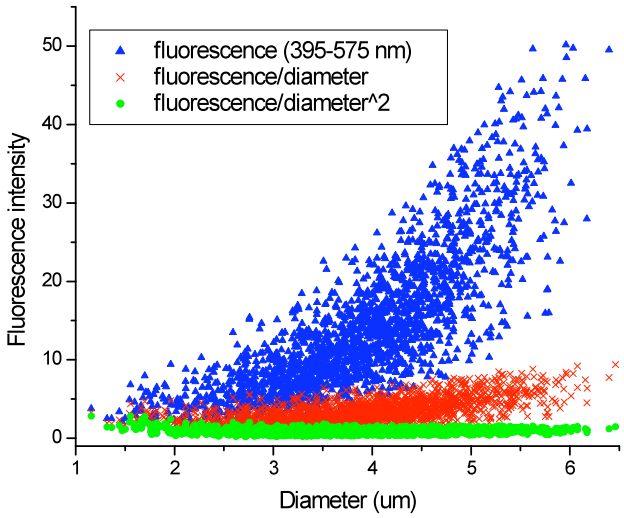

Fig. 21 Fluorescence, fluorescence/diameter, and fluorescence/diameter^2 varies with retinol (sample: PLGA_retinol_stag4_80-20b)

7. Summary

Previous UV-LIF measurements of homogeneous water droplets containing tryptophan (Hill et al, 2001) reveal the fluorescence intensity is approximately proportional to diameter squared. The tryptophan-loaded PLGA test samples herein exhibit a dependence of the fluorescence intensity on size somewhere between particle diameter and diameter squared. Smaller tryptophan-loaded PLGA particles appear more uniformly loaded than larger tryptophan-loaded PLGA particles. Further, the riboflavin and retinol loaded PLGA particles appear to have better uniformity of loading than the tryptophan-loaded PLGA particles.

References

Bottiger, J.R., Deluca, P.J., Stuebing, E.W., Vanreenaen, D.R., 1998. An ink jet aerosol generator. Journal of Aerosol Science 29 (Suppl. 1), S965.

Hill, S.C., Pinnick, R.G., Pan, Y.L., Holler, S., Chang, R.K., Bottiger, J.R., Chen, B.T., Orr, C.-S., Feather, G., 1999. Real-time measurement of fluorescence spectra from single airborne biological particles. Field Analytical Chemistry and Technology 3, 221–239.

Hill, S.C., Pinnick, R.G., Niles, S., Fell, N.F., Pan, Y.L., Bottiger, J., Bronk, B.V., Holler, S., Chang, R.K., 2001. Fluorescence from air-borne microparticles: dependence on size, concentration of fluorophores, and illumination intensity. Applied Optics 40, 3005–3013.
Lakowicz, J.R., 1983. Principles of Fluorescence Spectroscopy. Plenum Press, New York, NY.

Pan, Y.L., Cobler, P., Rhodes, S., Potter, A., Chou, T., Holler, S., Chang, R.K., Pinnick, R.G., Wolf, J.P., 2001. High-speed, high-sensitivity aerosol fluorescence spectrum detection using a 32-anode photomultiplier tube detector. Review of Scientific Instruments 72, 1831–1836.

Pan, Y.L., Holler, S., Chang, R.K., Hill, S.C., Pinnick, R.G., Niles, S., Bottiger, J.R., 1999. Single-shot fluorescence spectra of individual micrometer-sized bioaerosols illuminated by a 351-or 266-nm ultraviolet laser. Optics Letters 24, 116–118.

Pan, Y.L., Hartings, J., Pinnick, R.G., Hill, S.C., Halverson, J., Chang, R.K., 2003a. Single-particle fluorescence spectrometer for ambient aerosols. Aerosol Science and Technology 37, 628–639.

Pinnick, R.G., Hill, S.C., Nachman, P., Pendleton, J.D., Fernandez, G.L., Mayo, M.W., Bruno, J.G., 1995. Fluorescence particle counter for detecting airborne bacteria and other biological particles. Aerosol Science and Technology 23, 653–664.

Pinnick, R.G., Hill, S.C., Nachman, P., Videen, G., Chen, G., Chang, R.K., 1998. Aerosol fluorescence spectrum analyzer for rapid measurement of single micrometer-sized airborne particles. Aerosol Science and Technology 28, 95–104.

Pinnick, R.G., Hill, S.C., Pan, Y.-L., and Chang, R.K, 2003. Fluorescence spectra of atmospheric aerosol at Adelphi, Maryland, USA; measurement and classification of single particles containing organic carbon. Atmos. Environ., vol 38, 1657-1672 (2004).

Appendix B

TLS spectra are shown for potential fluorescent simulant material and bio-threat agents. Tryptophan was selected as a universal simulant.

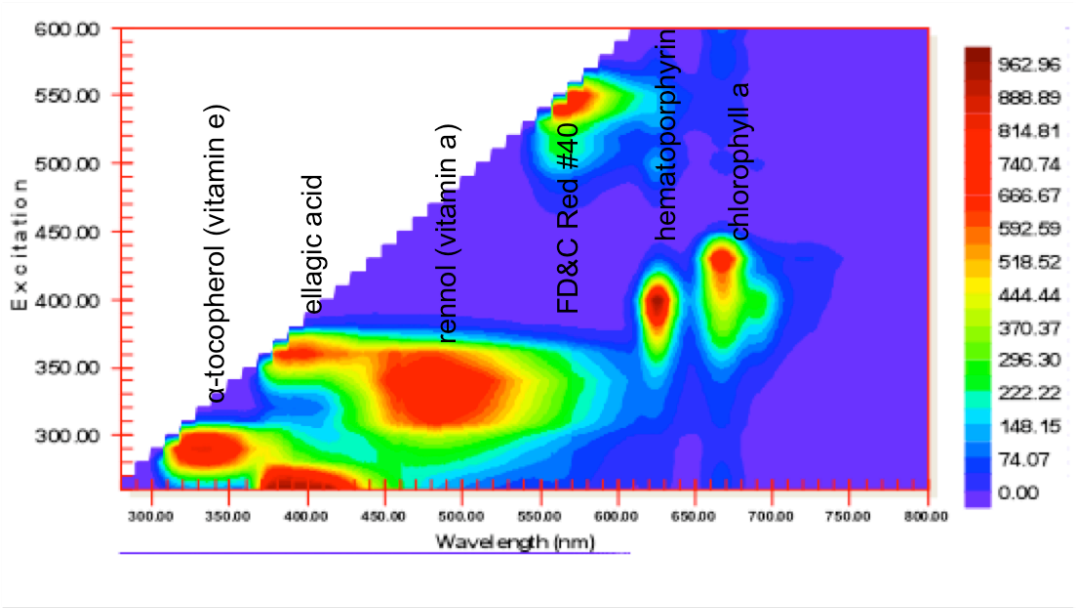

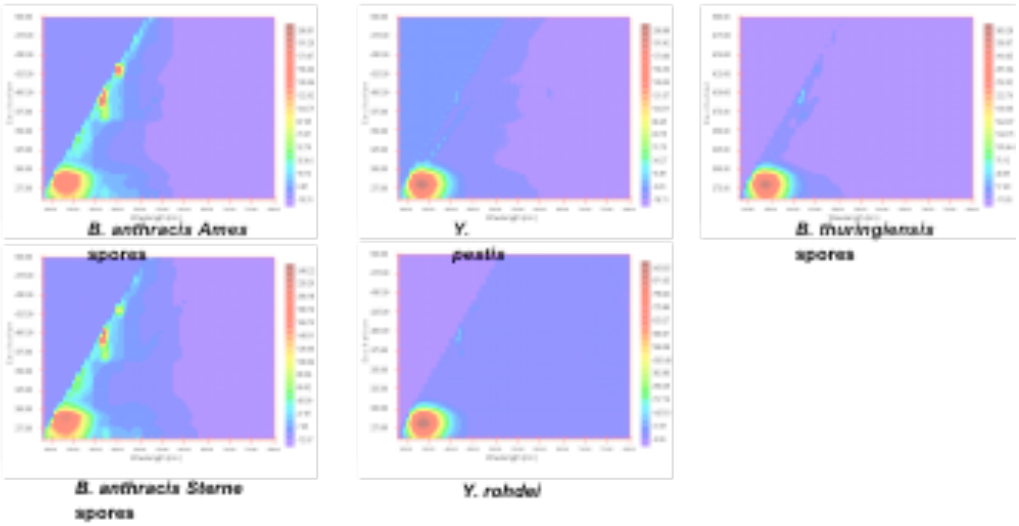

Appendix C

DEPARTMENT OF DEFENSE
PENTAGON FORCE PROTECTION AGENCY
9000 DEFENSE PENTAGON
WASHINGTON, DC 20301-9000

March 13, 2009

Dr. Jonathan Kaufman
Defense Threat Reduction Agency
8725 John J. Kingman Road
Ft. Belvoir, VA 22060

Dear Dr. Kaufman,

I am writing this letter in strong support of the biosimulant work of Dr. George Farquar, Lawrence Livermore National Laboratory, in the hope that this may encourage DTRA to support his efforts.

The Pentagon Force Protection Agency has implemented Pentagon Shield as a robust CBR detection and protection system. Throughout the system's development, data and testing have driven its design. However, efforts to thoroughly test the transport and dispersion of biological material, while successful, have been inherently limited by the number of biological simulants available. As the rollout and refinement of the system continues, the need for a safe simulant that would allow for numerous end-to-end system tests under realistic building conditions is greater than ever.

It was with great excitement that we saw Dr. Farquar's poster at the 2009 DHS Chemical and Biological Technologies Conference. His work offers the properties for a near ideal biosimulant, such as the low cost, food-safe nature critical to indoor testing efforts, the quantities available for said testing, aerodynamic suitability for dispersion testing, multiple, customizable, detectable tags, and sampling and detection system compatibility.

Therefore, we strongly support Dr. Farquar's work. We have an immediate need for these materials and look forward to serving as a test bed for their development. It is our opinion that this simulant will not only support our mission, but will provide invaluable data and opportunities to the field at large in the near term.

We would be happy to discuss our needs with you further and would be very interested in any possible collaboration on this project. If we may assist in any additional way, please contact my Deputy, Dr. Christina Murata, at 703-695-7476 or Christina.Murata@pfpa.mil.

Sincerely,

Paul Benda
Director, Chemical Biological
Radiological Nuclear and Explosives
Directorate